

Stochastic Ground Motion Simulation for Crustal Earthquakes in Japan

Tatsuya Itoi

Associate Professor, Graduate School of Engineering, the University of Tokyo, Tokyo, Japan

ABSTRACT: In this study, an empirical simulation model of stochastic ground motion for crustal earthquakes in Japan is proposed based on the ground motion records observed by K-NET in Japan from 1997 to 2011. The proposed model is developed based on that by Rezaeian & Der Kiureghian (2010). The characteristics of ground motion depends on various parameters such as magnitude, distance from source to site and local site conditions (shallow soil as well as deep subsurface structure), which is included in the parameters in the proposed model. The proposed model is considered useful when conducting probabilistic risk analysis of structures such as base-isolated or vibration-controlled buildings.

1. INTRODUCTION

For probabilistic seismic risk analysis of structure such as base-isolated or vibration-controlled structures, time history analysis is employed. Ground motion time history is needed for the analysis. For conventional seismic risk analysis, artificially-generated ground motion time history where amplitude is adjusted so that it fits ground motion intensity with some exceedance probability is used. Exceedance probability of the ground motion intensity measure for amplitude adjustment is obtained based on probabilistic seismic hazard analysis for the intensity measure. The ground motion parameter such as its duration, however, is conservatively assumed frequently, which prevents realistic estimate by overestimating or underestimating the risk of the structure.

On the other hand, ground motion simulation considering the fault rupture process such as the empirical Green's function method is widely used. It is, however, not appropriate to be utilized in probabilistic seismic hazard analysis. This is because it requires much time and resource as well as because there is no established method for variability in simulated ground motion.

Therefore, in this study, an empirical simulation model for ground motion time history is developed based on that proposed by Rezaeian & Der Kiureghian (2008, 2010), and an empirical attenuation relation of ground motion time history is proposed, based on the observed records by K-NET in Japan.

2. MODELLING OF GROUND MOTION

2.1. Overview

In this study, a model for velocity time history of ground motion is developed based on Rezaeian & Der Kiureghian (2008, 2010). Velocity time history $v(t)$ is assumed as follows:

$$v(t) \propto q(t, \boldsymbol{\alpha})u_0(t) \quad (1)$$

where, $q(t, \boldsymbol{\alpha})$ is a time modulating function and $u_0(t)$ is the stochastic process where variance is constant in time. The gamma distribution is employed for the time modulating function $q(t, \boldsymbol{\alpha})$ as follows:

$$q(t, \boldsymbol{\alpha}) \propto t^{\alpha_1} \exp(-\alpha_2 t) \quad (2)$$

where, α_1 and α_2 are the constants. These constants are determined by determining t_p , the time where the amplitude of envelope reaches maximum, and t_d , the time where the amplitude

of envelope becomes 0.1 times the maximum amplitude.

The amplitude of velocity time history $v(t)$ is defined by integrated squared velocity I_V as follows:

$$I_V = \int_0^{\infty} v^2(t) dt \quad (3)$$

The stochastic process $u_0(t)$ in Equation (1) is modelled by the weighted average of two stochastic processes, $u_1(t)$ and $u_2(t)$, as follows:

$$u_0(t) = \sqrt{r(t)}u_1(t) + \sqrt{(1-r(t))}u_2(t) \quad (4)$$

where, the direct S waves are modeled using $u_1(t)$, while the later phases are modeled using $u_2(t)$. The stochastic process, $u_1(t)$ and $u_2(t)$, respectively are modeled as the response of 1 DOF system with different natural frequency f_k and damping coefficient ζ_k which is excited by Gaussian process $w_k(\tau)$ as follows:

$$u_k(t) \propto \int_{-\infty}^t h_k(t-\tau|f_k, \zeta_k)w_k(\tau)d\tau \quad (5)$$

The weight $r(t)$ in Equation (4) is assumed proportional to time t as follows:

$$r(t) = \begin{cases} 1 - \frac{t}{t_c} & (0 < t \leq t_c) \\ 0 & (t > t_c) \end{cases} \quad (6)$$

The model proposed here needs eight parameters, I_V , f_1 , f_2 , ζ_1 , ζ_2 , t_c , t_p , t_d , to simulate velocity time history of ground motion.

2.2. Ground motion parameters

Ground motion parameters, I_V , f_1 , f_2 , ζ_1 , ζ_2 , t_c , t_p , t_d , are estimated for each recorded ground motion time history. The procedure for parameter estimation is almost same as that in Rezaeian & Der Kiureghian (2008, 2010).

3. GROUND MOTION DATABASE

Database for ground motion time histories recorded at K-NET stations at fault distances less than 100 km is compiled from crustal earthquakes of moment magnitude (M_w) larger than 5, which occurred from 1997 to 2011. Figure 1 shows the location of earthquake hypocenter, while the relation between magnitude and fault distance for

each record is shown in Figure 2. The range of site condition for recorded motions is $200\text{m/s} \leq V_{S30} \leq 700\text{m/s}$ and $Z_{1500} \leq 2000\text{m}$.

Ground motion parameters, I_V , f_1 , f_2 , ζ_1 , ζ_2 , t_c , t_p , t_d , are estimated for each component record.

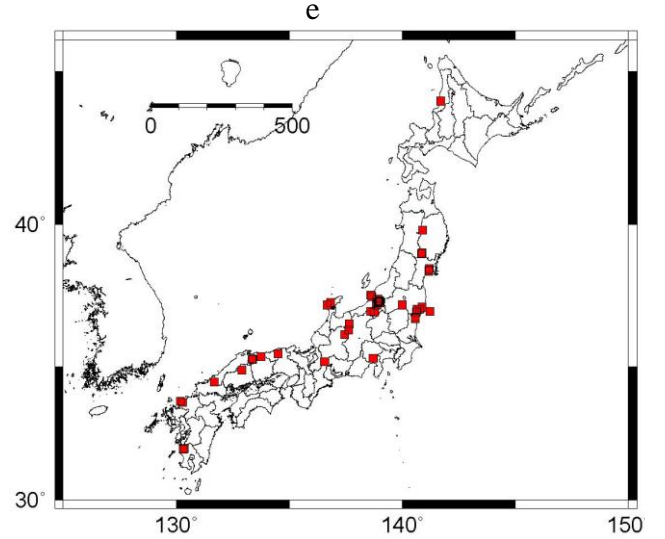


Figure 1: Location of earthquake hypocenter

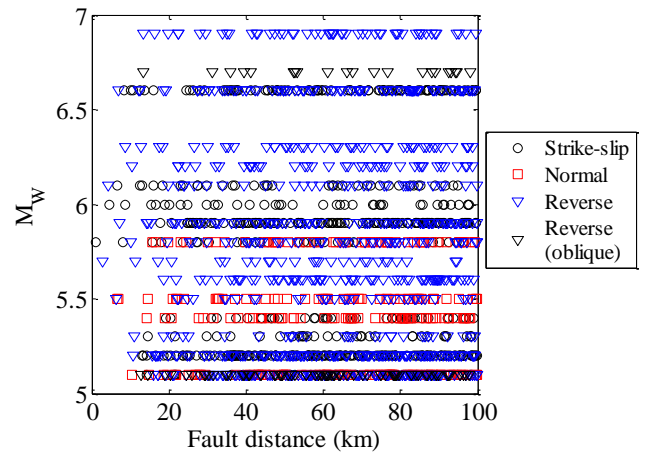


Figure 2: Relation between magnitude and fault distance for ground motion database

4. PREDICTION EQUATION

4.1. Transformation of probability distribution for ground motion parameters

First, statistics for each ground motion parameters are analyzed. Table 1 shows the probability

distribution and its parameters for each ground motion parameter. Table 1 shows the parameters for probability distribution for each ground motion parameter estimated by the maximum likelihood method.

Table 1: Parameter values.

Parameter	(unit)	Distribution	Bound	Distribution parameters			
I_v (v_1)	(m ² /s)	Lognormal	(0, ∞)	$\mu_{\ln Ev}$	-8.308	$\sigma_{\ln Ev}$	2.777
f_1 (v_2)	(Hz)	Gamma	(0, ∞)	α_{η}	4.549	β_{η}	0.8055
f_2 (v_3)	(Hz)	Gamma	(0, ∞)	α_{ρ}	1.597	β_{ρ}	1.328
ζ_1 (v_4)	-	Beta	(0, 1)	$q_{\zeta 1}$	1.0147	$r_{\zeta 1}$	5.484
ζ_2 (v_5)	-	Beta	(0, 1)	$q_{\zeta 2}$	0.8117	$r_{\zeta 2}$	2.553
t_c (v_6)	(s)	Gamma	(0, ∞)	α_{tc}	3.707	β_{tc}	5.143
t_p (v_7)	(s)	Gamma	(0, ∞)	α_{tp}	1.415	β_{tp}	3.226
$t_d - t_p$ (v_8)	(s)	Lognormal	(0, ∞)	$\mu_{\ln(td-tp)}$	3.488	$\sigma_{\ln(td-tp)}$	0.8019

Then, each ground motion parameter is transformed so that it fits the standard normal distribution as follows:

$$v_i = \Phi^{-1}(F_{\theta_i}(\theta_i)) \quad (7)$$

where, $\Phi^{-1}(\cdot)$ is the inverse of the standard normal distribution. The probability density function for the gamma distribution is as follows:

$$f_X(x) = \frac{1}{\beta^\alpha \Gamma(\alpha)} x^{\alpha-1} e^{-\frac{x}{\beta}} \quad (8)$$

where, the α and β are distribution parameters, and $\Gamma(\cdot)$ is the gamma function. The probability density function for the beta distribution is as follows:

$$f_X(x) = \frac{1}{B(q, r)} x^{q-1} (1-x)^{r-1} \quad (9)$$

where, and q and r are the distribution parameters, and $B(\cdot)$ is the beta function. The probability density function for the lognormal distribution is as follows:

$$f_X(x) = \frac{1}{x\sigma_{\ln X}\sqrt{2\pi}} \exp\left\{-\frac{(\ln x - \mu_{\ln X})^2}{2\sigma_{\ln X}^2}\right\} \quad (10)$$

where, $\mu_{\ln X}$ and $\sigma_{\ln X}$ are the distribution parameters.

Mean ground motion parameters v_{AMi} , which are the average of those for each component, v_{NSi} and v_{EWi} , is calculated as follows:

$$v_{AMi} = \frac{1}{2}(v_{NSi} + v_{EWi}) \quad (11)$$

Standard deviation of $v_{NSi} - v_{AMi}$ is estimated as follows:

$$\sigma_{comp i} = \sqrt{\text{Var}(v_{NSi} - v_{AMi})} \quad (12)$$

Table 2 shows the estimated standard deviation for each ground motion parameter.

Table 2: Standard deviation of $v_{NSi} - v_{AMi}$

v_1	v_2	v_3	v_4	v_5	v_6	v_7	v_8
0.083	0.385	0.194	0.569	0.389	0.627	0.311	0.233

4.2. Prediction equation

In this section, a prediction equation for each ground motion parameter is obtained. The explanatory variables for the equation are those for source, propagation path and site amplification characteristics as follows:

$$v_{AMijk} = g(M_{Wj}, D_j, R_{jk}, V_{S30k}, Z_{1500k}) + \varepsilon_{jk} \quad (13)$$

where, M_{Wj} , D_j , R_{jk} , V_{S30k} and Z_{1500k} are moment magnitude, hypocenter depth, shortest fault distance, 30 meter average shear wave velocity and depth to the layer with shear wave velocity of 1500m/s.

The regression equation for each ground motion parameter is as follows:

$$\begin{aligned} v_{AM1} &= a_{10} + a_{11} \frac{M_W}{6.0} + a_{12} \frac{D}{10\text{km}} \\ &+ a_{13} \log_{10} \left(\frac{R + a_{16} 10^{a_{17} M_W}}{40\text{km}} \right) \\ &+ a_{14} \log_{10} \left(\frac{V_{S30}}{400\text{m/s}} \right) \\ &+ a_{15} \frac{\min(Z_{1500}, a_{i9})}{100\text{m}} + \varepsilon_1 \end{aligned} \quad (14)$$

$$\begin{aligned} v_{AMi} &= a_{i0} + a_{i1} \frac{M_W}{6.0} + a_{i2} \frac{D}{10\text{km}} + a_{i3} \frac{R}{40\text{km}} \\ &+ a_{i4} \log_{10} \left(\frac{\min(V_{S30}, a_{i8})}{400\text{m/s}} \right) \\ &+ a_{i5} \log_{10} \left(\frac{Z_{1500}}{100\text{m}} \right) + \varepsilon_i \quad (i = 2, 3) \end{aligned} \quad (15)$$

$$v_{AMi} = a_{i0} + a_{i1} \frac{M_W}{6.0} + a_{i2} \frac{D}{10\text{km}} + a_{i3} \frac{R}{40\text{km}} + a_{i4} \log_{10} \left(\frac{V_{S30}}{400\text{m/s}} \right) + a_{i5} \frac{Z_{1500}}{100\text{m}} + \varepsilon_i \quad (i = 4,5,7) \quad (16)$$

$$v_{AMi} = a_{i0} + a_{i1} \frac{M_W}{6.0} + a_{i2} \frac{D}{10\text{km}} + a_{i3} \frac{\min(R, a_{i6})}{40\text{km}} + a_{i4} \log_{10} \left(\frac{V_{S30}}{400\text{m/s}} \right) + a_{i5} \frac{\min(Z_{1500}, a_{i9})}{100\text{m}} + \varepsilon_i \quad (i = 6,8) \quad (17)$$

The regression results and the standard deviation of residuals are shown in Table 3, while the correlation coefficients between residuals are shown in Table 4.

4.3. Simulation of ground motion by proposed equations

Ground motion time history of north-south component is simulated using the proposed equations. Figure 3 shows some samples for velocity and acceleration time histories for simulated ground motions. Ground motions are simulated for the source with $M_W=6.5$, $D=15\text{km}$ and the site for $R=10\text{km}$, $Z_{1500}=1000\text{m}$, $V_{S30}=500\text{m/s}$.

Figure 3 shows the comparison with respect to acceleration response spectra between the simulated ground motions and existing attenuation equations. Simulated acceleration response spectra are higher in the short period range. Effects of deep subsurface structure are simulated by the proposed model, while existing attenuation equations do not. Figure 4 shows the amplification of response spectrum ($T=2\text{s}$) due to deep subsurface structure, which is harmonic with the existing empirical relationship proposed by Itoi & Takada (2012).

Table 3: Regression coefficients and standard deviation of prediction error for Equations (14) – (18)

GMP	a_{i0}	a_{i1}	a_{i2}	a_{i3}	a_{i4}	a_{i5}	a_{i6}	a_{i7}	a_{i8}	a_{i9}	σ_{ε_i}
I_V v_{GM1}	-8.046	8.400	0.254	-2.193	-1.498	0.099	31.65	0.394	-	444.1	0.386
f_1 v_{GM2}	3.022	-3.248	0.163	0.207	0.914	-0.330	-	-	393.9	-	0.863
f_2 v_{GM3}	3.558	-3.212	0.301	-0.121	2.371	-0.673	-	-	253.6	-	0.718
ζ_1 v_{GM4}	-1.460	2.015	-0.133	-0.161	1.499	-0.009	-	-	-	-	0.851
ζ_2 v_{GM5}	-0.640	0.807	-0.144	0.096	2.099	-0.021	-	-	-	-	0.803
t_c v_{GM6}	-3.726	2.215	-0.054	0.730	-0.712	0.118	65.77	-	-	664.0	0.934
t_p v_{GM7}	-4.885	4.706	-0.315	0.303	-0.527	0.051	-	-	-	-	0.690
t_d-t_p v_{GM8}	-3.865	2.116	-0.263	1.432	-0.648	0.185	48.81	-	-	640.0	0.723

Table 4: Correlation coefficients between prediction errors for Equations (14) – (18).

	v_{GM1}	v_{GM2}	v_{GM3}	v_{GM4}	v_{GM5}	v_{GM6}	v_{GM7}	v_{GM8}
v_{GM1}	1	-0.229	0.061	-0.075	-0.311	-0.162	0.008	-0.203
v_{GM2}		1	0.332	-0.338	0.287	-0.027	-0.006	-0.072
v_{GM3}			1	-0.134	-0.221	-0.176	-0.227	-0.537
v_{GM4}				1	0.157	-0.181	0.068	0.103
v_{GM5}					1	0.010	-0.139	-0.039
v_{GM6}			sym.			1	0.109	0.444
v_{GM7}							1	0.330
v_{GM8}								1

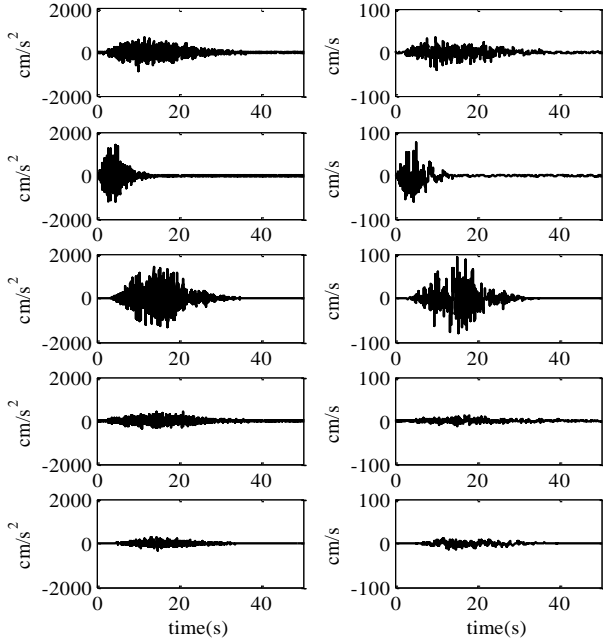


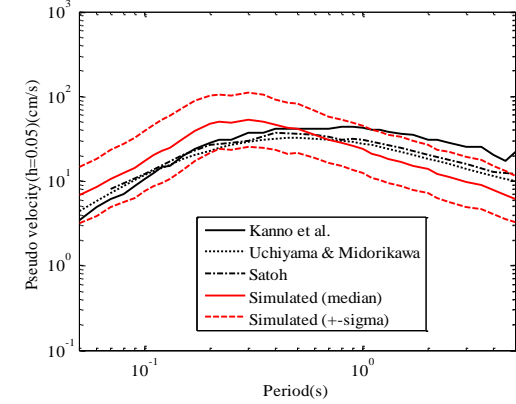
Figure 3: Samples of simulated ground motions
 (north-south component)
 ($M_W=6.5$, $D=15\text{km}$ and the site for $R=10\text{km}$,
 $Z_{1500}=1000\text{m}$, $V_{S30}=500\text{m/s}$)

5. CONCLUSIONS

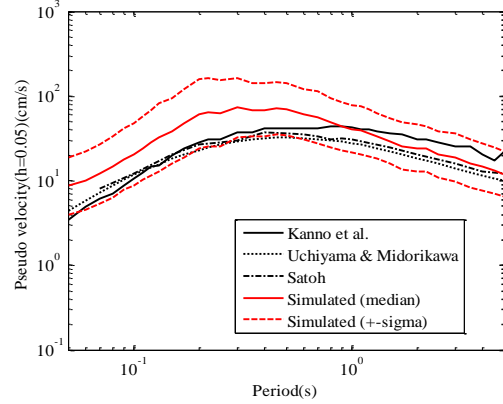
In this study, an attenuation relation for velocity ground motion time history is proposed for crustal earthquake in Japan. The proposed model is harmonic with existing attenuation relation for acceleration response spectra. The proposed relation can be applied to crustal earthquake with $5.1 \leq M_W \leq 6.9$, and at the site for the shortest distance $R \leq 100\text{km}$ and the soil condition $200\text{m/s} \leq V_{S30} \leq 700\text{m/s}$ and $Z_{1500} \leq 2000\text{m}$. The proposed model, however, is not applicable to the near-field ground motion at a soft soil site, because the non-linearity of soil amplification is not included in the proposed model, which will be discussed in the future study.

6. ACKNOWLEDGEMENT

Ground motion data are provided by NIED (K-NET).



(a) $R=10\text{km}$ $Z_{1500}=20\text{m}$



(b) $R=10\text{km}$ $Z_{1500}=1000\text{m}$

Figure 4: Comparison between simulated ground motions and conventional attenuation relation for response spectra

($M_W=6.5$, $D=15\text{km}$, $V_{S30}=500\text{m/s}$)

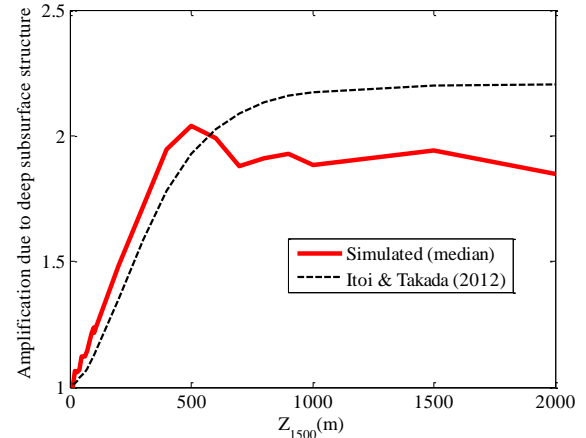


Figure 5: Amplification for $Sa(T=2\text{s})$ due to deep subsurface structure

($M_W=6.5$, $D=15\text{km}$, $V_{S30}=500\text{m/s}$)

7. REFERENCES

- Itoi, T. & Takada, T. (2012). "Empirical correction of ground motion prediction equations of response spectra at rock sites for near-field earthquakes considering amplification effect with deep subsurface structure", *Journal of Japan Association for Earthquake Engineering*, 12(1), 1_43-1_61. (in Japanese)
- Kanno, T. et al. (2006). "A New Attenuation Relation for Strong Ground Motion in Japan Based on Recorded Data" *Bulletin of the Seismological Society of America*, 96(3), 879–897.
- Rezaeian & Der Kiureghian (2008). "A stochastic ground motion model with separable temporal and spectral nonstationarities", *Earthquake Engineering and Structural Dynamics*, 37(13), 1565-1584.
- Rezaeian & Der Kiureghian (2010). "Simulation of synthetic ground motions for specified earthquake and site characteristics", *Earthquake Engineering and Structural Dynamics*, 39(10), 1155-1180.
- Satoh, T. (2008). "Attenuation relations of horizontal and vertical ground motions for P wave, S wave, and all duration of crustal earthquakes" *Journal of structural and construction engineering* 73(632), 1745-1754 . (in Japanese)
- Uchiyama, Y. & Midorikawa, S. (2006). "Attenuation relationship for response spectra on engineering bedrock considering effects of focal depth" *Journal of structural and construction engineering* (606), 81-88. (in Japanese)